Algorithm Theoretical Basis Document

for

Brightness Temperature

Version 3.1 July 23, 2001

Ronald E. Alley
Marit Jentoft-Nilsen
Jet Propulsion Laboratory
4800 Oak Grove Drive
Pasadena, CA 91109

1.0 Introduction

The Advanced Spaceborne Thermal Emission and Reflectance Radiometer (ASTER) is a high-spatial-resolution multispectral imaging device that was launched in Earth orbit on December 18,1999, on TERRA, the first platform of NASA's Earth Observing System (EOS). The instrument has three bands in the visible and near infrared (VNIR) spectral range (0.5 to 1.0 μm) with 15 meter spatial resolution, six bands in the short-wave infrared (SWIR) spectral range (1.0 to 2.5 μm) with 30 meter spatial resolution, and five bands in the thermal infrared (TIR) spectral range (8 to 12 μm), with 90 meter spatial resolution (Kahle, et al., 1991; Yamaguchi, et al., 1993). An additional backward viewing telescope with a single band in the near infrared with 15 meter spatial resolution provides the capability, when combined with the nadir viewing elements, for same-orbit stereo data. The Japanese Government, under the Ministry of Trade and Industry (MITI) is providing the instrument. The ASTER project is implemented through the Earth Resources Satellite Data Analysis Center (ERSDAC) and the Japan Resources Observation System Organization (JAROS), which are nonprofit organizations under the control of MITI. JAROS is responsible for the design and development of the ASTER instrument, which was carried out by the Nippon Electric Company (NEC), the Mitsubishi Electric Corporation (MELCO), Fujitsu, and Hitachi under contracts with JAROS. The ASTER science team is an international team of Japanese, American, French, and Australian scientists. The team participates in the definition of the scientific requirements for ASTER, in the development of algorithms for data reduction and analysis, and in calibration, validation, and mission planning.

1.1 Algorithm Identification

This Algorithm Theoretical Basis Document (ATBD) describes the algorithm used to produce the brightness temperature at sensor product (ASTER product number AST04). This product is currently produced only for TIR data, although the algorithm could be adapted for SWIR data nighttime scenes containing elevated temperatures.

1.2 Data Product Name and Number

Brightness Temperature at Sensor, product number AST04

1.3 Document Scope

The purpose of this document is to describe both the theoretical basis and practical aspects of the brightness temperature algorithm in sufficient detail to allow the ASTER science team, Algorithm Review Board, and the user community to evaluate it. The document starts with a description of the general background of the algorithm and the basic

equation defining the relation between the input and output products. It then gives a detailed mathematical description of the algorithm used to solve the basic equation, including variance and uncertainty estimates. The final section discusses the practical and numerical considerations, including calibration and validation, programming considerations, diagnostics, exception handling, limitations, and assumptions. Included as an appendix is a chart of the ASTER Standard Product interdependencies.

2.0 Overview and Background Objective

2.1 Experimental Objective

ASTER is the only high spatial resolution surface-imaging instrument on the TERRA platform. As a result, there are a variety of unique science objectives that the instrument will be able to address. The main contributions to the EOS global change studies will be in providing surface temperatures, surface emitted and reflected radiance, cloud properties, and digital elevation models (DEMs) at a spatial scale that will allow detailed studies to be conducted.

TERRA carries two other surface imaging instruments in addition to ASTER. They are the Multi-angle Imaging Spectro-Radiometer (MISR) and the Moderate Resolution Imaging Spectrometer (MODIS). High spatial resolution data from ASTER are used to create datasets on a spatial scale of tens of meters. This data can be verified by field measurements, which, at the same time can be used to understand the averaged response of the instruments that have coarser spatial resolution. ASTER can study in more detail those quantities and processes (such as the surface properties, elements of the surface energy and water balance, and cloud properties) that are monitored globally by MODIS and/or MISR at a moderate resolution. Data from MODIS and MISR will be used to help with the atmospheric correction of ASTER data.

The objective of the algorithm described in this document is to convert the radiance values that have been observed by the sensor into the corresponding brightness temperature values. The brightness temperature product contains essentially the same information as the input radiance product, but in a form that is more easily and intuitively understood. Temperature units are almost universally familiar, while only a fraction of the potential user community has an intuitive grasp of radiance units.

Spectral emissivity variations are also more apparent in the brightness temperature product than in the radiance product. Since a particular pixel has a kinetic temperature, independent of wavelength, the deviations of the brightness temperature from band to band may be ascribed to spectral emissivity differences. The spectral emissivity curve for a pixel is essentially the inverse of the brightness temperature curve. The user can therefore readily find features of spectral emissivity by inspection of the brightness temperature values.

2.2 Historical Perspective

The radiance perceived by a sensor is a function of the radiation emitted from the target and the radiation emitted and absorbed by the intervening atmosphere, integrated over the response function of the sensor. The radiation emitted from the target at a given wavelength is a function of its temperature and emissivity. Atmospheric effects are disregarded in the calculation of brightness temperature at the sensor, so we can say the radiance at the sensor is the integral over the instrument response function of the emissivity times the blackbody radiance. The temperature and the spectral emissivity are the unknowns in this equation. If we set the emissivity to one, we can calculate the remaining unknown, the temperature. Setting the emissivity to one is equivalent to assuming that the target is a blackbody, so the brightness temperature can be defined as the temperature that a blackbody would be in order to produce the radiance perceived by the sensor. Brightness temperature has been used to observe volcanic ash clouds (Prata, 1989) and detect ice leads in the Arctic (Stone, 1993) to name just a few examples.

2.3 Instrument Characteristics

ASTER provides data in three spectral regions using three separate radiometer subsystems. These are the visible and near-infrared (VNIR) subsystem being provided by NEC, the short wavelength infrared (SWIR) subsystem provided by MELCO, and the thermal infrared (TIR) subsystem provided by Fujitsu. The instrument bandpasses, radiometric accuracy, and radiometric and spatial resolution for the TIR and SWIR subsystems are given in Table 1. A wide dynamic range and multiple gain settings help ensure useful data for a variety of investigations. Current plans call for only TIR data to be used for input into the brightness temperature algorithm, although the algorithm could be expanded to include nighttime SWIR data at some future date.

The swath width is 60 kilometers for each of the three subsystems. The ASTER instrument has a crosstrack pointing capability of 8.55 degrees for the TIR and SWIR subsystems, which gives a crosstrack observational range of approximately 136 kilometers on the surface. Any point on the earth's surface (except the extreme polar regions) are accessible by the TIR and SWIR at least once every sixteen days.

Instrument and spacecraft resources are allocated to support an eight percent average duty cycle, which corresponds to over 700 60x60 kilometer scenes per day. ASTER data are acquired and processed according to specific user requirements that identify the acquisition time,

gain, wavelength region, and data product. In addition, ASTER has the goal of obtaining a cloud-free data set for the entire Earth's land surface by the end of its mission. Users will be able to request that data products, of local and regional extent, be made from the global data set. The stereo capability will be used to generate high-resolution digital elevation models (DEMs) in selected regions. Observations will also include sites involving highly coordinated field experiments with simultaneous ground and aircraft measurements, targets of opportunity such as volcanoes, fires and major weather events, and observations of clouds on a local to regional scale.

Table 1. Spectral and spatial characteristics of the ASTER TIR and SWIR instruments.

ASTER TIR and SWIR					
Wavelength Region	Band Number	Spectral Range (μm)	Radiometric Accuracy	Radiometric Resolution	Spatial Resolution
SWIR	4	1.60-1.70	± 4 %	≤ 0.5 %	30 m
	5	2.145-2.185	± 4 %	≤ 1.3 %	30 m
	6	2.185-2.225	± 4 %	≤ 1.3 %	30 m
	7	2.235-2.285	± 4 %	≤ 1.3 %	30 m
	8	2.295-2.365	± 4 %	≤ 1.0 %	30 m
	9	2.360-2.430	± 4 %	≤ 1.3 %	30 m
TIR	10	8.125-8.475	1-3 °K	≤0.3 °K	90 m
	11	8.475-8.825	1-3 °K	≤ 0.3 °K	90 m
	12	8.925-9.275	1-3 °K	≤ 0.3 °K	90 m
	13	10.25-10.95	1-3 °K	≤ 0.3 °K	90 m
	14	10.95-11.65	1-3 °K	≤ 0.3 °K	90 m

3 Algorithm Description

3.1 Theoretical Description

3.1.1 Physics of the Problem

The spectral radiance of a blackbody at temperature, T, and wavelength, λ, is given by the Planck function.

$$L_{\lambda}^{BB} = \frac{c_1}{\lambda^5 \pi \left[e^{\frac{c_2}{\lambda T}} - 1 \right]} \quad \textbf{(1)}$$

where:

L^{BB} = blackbody radiance (W-m^{-2}-steradian^{-1}-μ^{-1})
λ = wavelength (m)
T = temperature (°K)
C_1 = first radiation constant (3.741775x10^{-22} W-m^{3}-μ^{-1})
C_2 = second radiation constant (0.0143877 m-°K)

This equation is integrated over an instrument response function to calculate the radiance that corresponds to a brightness temperature for a particular instrument channel (band).

$$L_s = \frac{\int \psi(\lambda) L^{BB}(T, \lambda) d\lambda}{\int \psi(\lambda) d\lambda} \quad \textbf{(2)}$$

where:

L_s = radiance observed by the sensor
ψ = instrument response

A mathematical description of the technique to solve for temperature is provided below.

3.1.2 Mathematical Description of Algorithm Alternatives

The solution that we seek is the inverse of Equation 2. That is, we wish to compute temperature (T) as a function of sensor radiance (L_S). Unfortunately, for sensor response functions of finite (not infinitesimal) width, Equation 2 cannot be inverted explicitly. Several methods have been examined to approximate the solution of the inverse of Equation 2.

The most straightforward approximation is to replace the response function with a delta function at the sensor's central wavelength. Under this approximation Equation 2 collapses into Equation 1, which can be inverted to

$$T_c = \frac{c_2}{\lambda_c \log\left(\frac{c_1}{\lambda_c^5 \pi L_s} + 1\right)} \quad \textbf{(3)}$$

where:

T_c = brightness temperature, from a central wavelength

λ_c = the sensor's central wavelength

Implicit in the computation of a central wavelength for a TIR sensor is a standard temperature. Equation 3 is accurate for the observed radiance that yields the standard temperature, but it becomes increasingly inaccurate for temperatures farther away from the standard temperature.

Also considered was an alternative method that uses the result of the preceding technique as a first guess at the solution. The computed temperature is used to solve the right-hand side of Equation 2. For a set of calibrated sensor response values, Equation 2 becomes

$$L_c = \frac{\sum_i \psi_i \cdot L^{BB}(T_c, \lambda_i) \cdot \Delta\lambda}{\sum_i \psi_i \cdot \Delta\lambda} \quad \textbf{(4)}$$

where

L_c = computed radiance from the trial temperature

This computed radiance should ideally be equal to the observed sensor radiance. By adjusting the trial temperature in Equation 4, an iterative method can be established, which will converge upon the solution to any desired precision. This approach is, however, computationally time consuming.

The first method was ultimately rejected because of its inaccuracy. Variations of the second method were rejected on the basis of their computational demands.

3.1.3 Mathematical Description of the Algorithm

The algorithm that has been selected does not attempt an inversion of Equation 2 by making a simplifying approximation. Instead, Equation 2 is solved directly; the expected radiance at the sensor is computed at

finely spaced temperature intervals for the range of temperatures that the sensor is designed to receive. This results in a table of values that represent observed radiance as a function of brightness temperature for a given sensor. Rather than invert Equation 2, we invert the generated table (that is, form a new table from the old one, where brightness temperature is represented as a function of observed radiance). It is possible to invert this table to any desired precision by simply enlarging the original table to include a sufficient number of entries in the table. The generation and inversion of this table would be computationally expensive if it were required to be redone for each scene, but the results are constant for a given wavelength calibration of the sensors, and therefore, presumably, for the life of the mission. The table need be generated and inverted only once, prior to launch. Then, to generate the brightness temperature product for a given scene, one need only use the radiance value of each input pixel as the index to point to the desired brightness temperature in the stored table, and place the table values in the output dataset.

It would be instructive to show in detail how this table is generated and inverted. Doing this will not only clarify the technique used, but it will also illuminate the constraints that are needed to maintain precision.

The input dataset for this product is the radiance observed at the sensor, in units of Watts per square meter per steradian per micrometer. The input values are stored as twelve bit unsigned integer, and linear scaling factors are used to convert from the stored values to the designated units. The scaling factor for each band has been chosen to make the maximum reportable radiance to be equivalent to 370.0 degrees Kelvin, which is the maximum temperature that the TIR subsystem is designed to observe accurately. This data representation constrains the precision of the input data to be at best equivalent to 0.02 degrees Celsius.

The output product is reported in units of degrees Celsius, scaled by a factor of 100. For example, an output value of 2735 implies a brightness temperature of 27.35 degrees. The output values are thus reported to a precision of 0.01 degrees Celsius. Note, however, that the true precision is constrained by the input values to be 0.02 degrees Celsius, as stated above. Output values are stored as sixteen bit signed integers, permitting 65,536 possible output values.

To construct the table of radiance values as a function of brightness temperature and ASTER channel, Equation 4 is solved for the temperature values that span the range of possible observed radiance values. The temperature values used are in 0.010 degree increments, starting with -200.00 degrees Celsius, and increasing to +100.00 degrees

Celsius. These temperatures span the range of radiances that can be represented in the input.

To invert the table just described, each radiance value from 0.001 to 32.768 Watts per square meter per steradian per micrometer, in increments of 0.001 units is compared to the table values. Each radiance value will fall between two of the table entries; that radiance is then assigned the temperature (to the nearest 0.01 degree) of the closer radiance of those two entries. The resulting table will contain 2^{15} by 5 entries, with each entry a value that represents the temperature corresponding to that radiance and channel. The associated radiance values are implied by the location of each table entry. The table is permanently stored for later use in generating the brightness temperature product. When a brightness temperature product needs to be generated, the task is simply a matter of table lookup.

3.1.4 Variance and Uncertainty Estimates

The uncertainties introduced by this algorithm result from two sources: errors and uncertainties in the wavelength calibration of the instrument, and the rounding (digitization) error imposed by the method of storing the results.

The rounding errors should be uniformly distributed over the range ±0.005 degrees Celsius, yielding a standard deviation of 0.0029 degrees. The ASTER TIR design specification does not require a radiometric resolution better than 0.3 degrees. For a perfectly linear radiometric response over the specified temperature range for ASTER TIR, the 12 bit recording level of the instrument limits the resolution to no better than 0.02 degrees, under any conditions.

An assessment of the uncertainties of the wavelength calibration is less definitive, but a few general comments can be stated. The brightness temperature results will be fairly insensitive to random errors (errors in the shape of the response function), but more sensitive to any bias (errors in the central wavelength value). As a crude rule of thumb, a 5 nanometer (0.005 micrometer) error in the central wavelength is required to produce a 0.02 degree error in the calculated brightness temperature. The wavelength calibration is not expected to be a major source of error (uncertainty) in the results of this product.

In conclusion, it is assumed that the largest source of uncertainty in the output values will be the corresponding uncertainty of the input values.

3.2 Practical Considerations

3.2.1 Programming / Procedural Considerations

The radiance to temperature lookup table is presently implemented as a separate file, which is read by the brightness temperature software each time an ASTER brightness temperature product is generated. Alternatively, the lookup table could be included as part of the program software itself. This would result in a slight gain of execution speed, at a small cost to the clarity of the software. This alternative is not expected to be used unless program execution speed becomes an overwhelming issue.

The software delivery for this product includes the lookup table, rather than the software to generate the lookup table.

This approach is well suited to potential parallel processing implementations, since the lookup on each pixel is independent of any other pixel's value.

3.2.2 Calibration and Validation

The output temperature value for a pixel depends upon two values, the input radiance value, and the sensor spectral response function. The radiance calibration is discussed in the ATBD for the Level 1B product, "Radiance at Sensor - TIR". The pre-launch calibration of the sensor spectral response functions has been carried out by Fujitsu, the manufacturer of the TIR subsystem. A full post-launch verification of the pre-launch calibration is not feasible, but the ASTER data acquired for post-launch validation of the Level 1B product has been examined to verify that it is consistent with the pre-launch calibration.

The primary validation concern for this product is one of software testing. Has the lookup table been constructed properly, and does the associated computer program manipulate the input data and the lookup table correctly? To assure proper operation, the brightness temperature product was generated for several scenes of ASTER data. The results were compared to results obtained from independently created software. The products generated by the two different techniques produce the same results.

3.2.3 Quality Control and Diagnostic Information

Quality control on this product is more an assessment of the input data (radiance products and the instrument response functions used to calculate the lookup table) than of the algorithm itself. The quality control and diagnostic information that are produced and appended to

this product consists of a histogram of the brightness temperature values (1 °C intervals with a range -100 to +100 °C).

In addition, all ASTER Level 2 products contain a pixel map in a format common to all of the products. This map will identify any pixels that are known to be defective, and report the nature and severity of the defect. The map also notes the presence of clouds in the pixel, to the extent that this information is known.

3.2.4 Exception Handling

No attempt will be made to calculate the brightness temperature for pixels that have been previously identified as:

1) Dropped lines
2) Dropped pixels
3) Invalid data

These values will be replaced with a predetermined replacement value for "bad" pixels.

4.0 Constraints, Limitations, Assumptions

At present there are no known constraints on the algorithm that would prevent it from producing a valid output product from any valid input thermal radiance image.

The conversion from radiance to temperature is performed only upon those pixels for which the input radiance is a positive value. All other pixels will be marked upon output as invalid data.

The algorithm is based upon the assumption that the ASTER TIR subsystem sensor response calibration is accurate. This appears to be true.

Brightness temperature is defined as the temperature that a blackbody would have in order to produce the observed radiance. If one considers a brightness temperature to be the surface temperature, that person has assumed that the atmospheric path has had no effect on the radiance value, and that the surface is emitting as a blackbody (i.e., with a spectral emissivity of 1.0 at all wavelengths).

5.0 References

Fujisada, H., and Ono, A. 1993. Anticipated performance of the ASTER instrument in EM design phase. *SPIE Proceedings*. pp. 187-197.

Kahle, A. B., Madura, D. P., and Soha, J. M. 1980. Middle Infrared Multispectral Aircraft Scanner Data Analysis for Geological Applications. *Applied Optics*, vol. 19, pp. 2279-90.

Kahle, A. B., Palluconi, F. D., Hook, S. J., Realmuto, V. J., and Bothwell, G. 1991. The Advanced Spaceborne Thermal Emission and Reflectance Radiometer (ASTER), *International Journal of Imaging Systems and Technology*, vol. 3, pp. 144-156.

Palluconi, F. D., and Meeks, G. R., 1985. *Thermal Infrared Multispectral Scanner (TIMS): An Investigator's Guide to the Data,* JPL Publication 85-32.

Planck, M. 1901. On the Distribution of Energy in the Spectrum. *Ann. Phys.*, vol. 4, no. 3, pp. 553-563.

Prata, A. J. 1989. Observations of volcanic ash clouds in the 10-12 μm window using AVHRR/2 data. *International Journal of Remote Sensing*, vol. 10, nos. 4 and 5, pp. 751-761.

Sabins, Jr, F. F. 1978. *Remote Sensing Principles and Interpretation.* W. H. Freeman and Company, San Francisco, 426p.

Siegal, R. and Howell, J. R. 1982. *Thermal Radiation Heat Transfer: Second Edition*, Hemisphere Publishing Corporation, New York.

Stone, R. S. 1993. The Detectability of Arctic Leads using Thermal Imagery under varying Atmospheric Conditions. J*ournal of Geophysical Research - Oceans*, vol. 98, no. nc7, pp. 12469-12482.

Yamaguchi, Y., Tsu, H., and Fujisada, H. (1993). A scientific basis of ASTER instrument design. *SPIE Proceedings*, pp 150-160

ASTER Product Inter-Dependencies

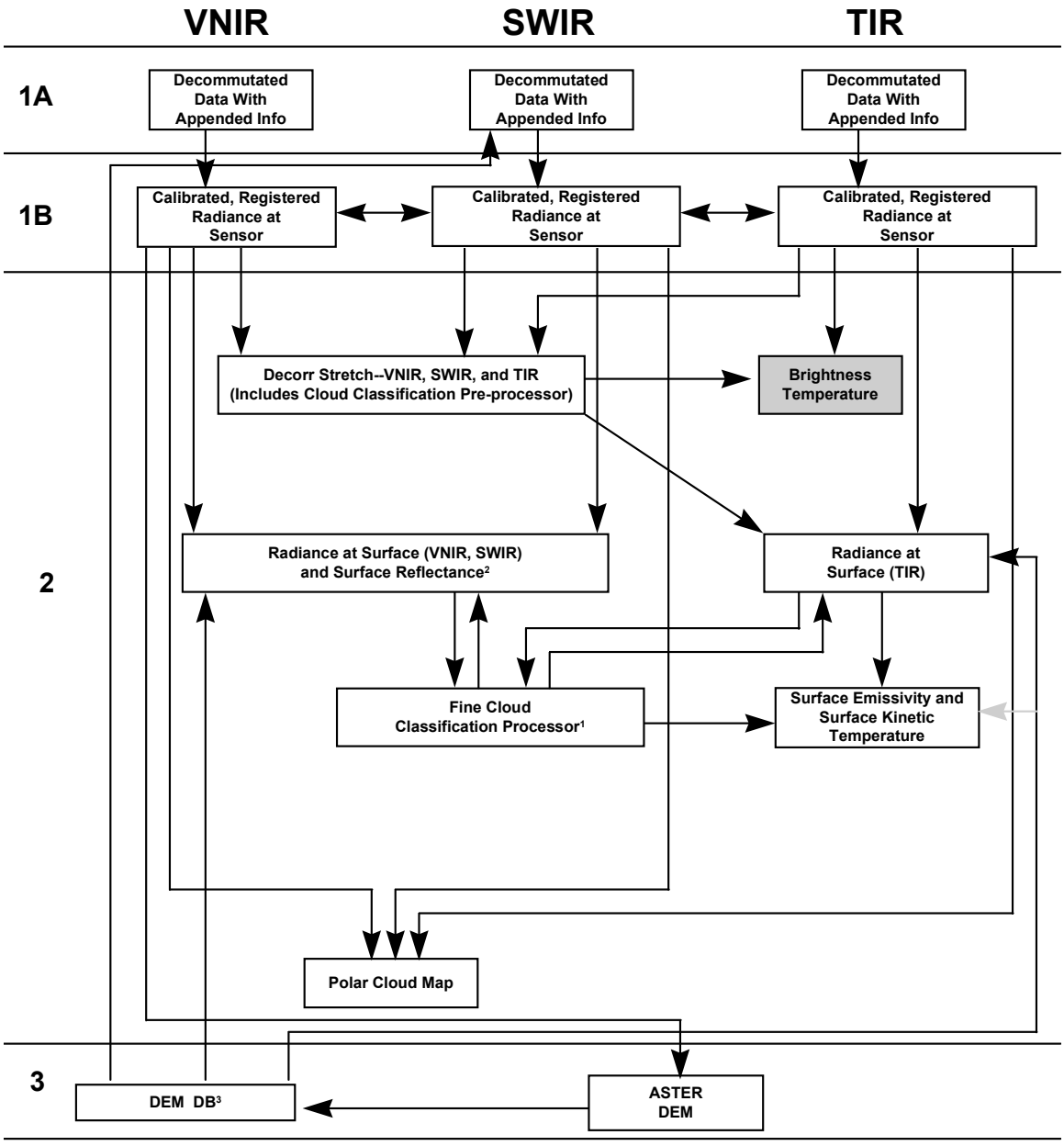

[1]Produces a cloud mask that is incorporated into other products
[2]Computed simultaneously with Radiance at Surface
[3]Refers to a database of DEM data regardless of the source